

Spectroscopic (FT-IR, FT-Raman and NMR) investigations, quantum chemical studies, Fukui function, magnetic susceptibility, HOMO-LUMO, NBO, and NLO properties of 4-nitrophenyl)ethanone

M. Karunanidhi¹, V. Balachandran^{2,*}, B. Narayana³, K. Anitha⁴ and M. Karnan¹

¹Department of Physics, Srimad Andavan Arts and College (Autonomous), Tiruchirappalli-620 005, India.

²Centre for Research, Department of Physics, A.A. Government Arts College, Musiri-621 211, India.

³Department of Studies in Chemistry, Mangalore University, Mangalagangothri-574 199, India.

⁴Department of Physics, Bharathidasan University Constituent College, Lalgudi, Tiruchirappalli- 621 601, India.

ARTICLE INFO

Article history:

Received: 25 March 2017;

Received in revised form:
25 April 2017;

Accepted: 8 May 2017;

Keywords

Fukui function,
Magnetic susceptibility,
NLO,
1(4-Nitrophenyl) ethanone,
MEP,
Thermodynamic properties.

ABSTRACT

The FT-IR, FT-Raman spectra of 1(4-nitrophenyl)ethanone (NPE) were recorded in the region 4000-400 cm^{-1} and 4000-100 cm^{-1} and analyzed. Optimized molecular structure, vibrational wavenumbers, corresponding assignments regarding NPE has become screened tentatively as well as hypothetically using Gaussian 09 program package. The geometrical parameters of the title compound are in agreement with the experimental data. Natural bonding orbital (NBO) assessment has been completed with a reason to clarify charge transfer or conjugative interaction, the intramolecular re-hybridization and delocalization of electron density within the molecule. From the MEP analysis, it is clear that the negative electrostatic potential regions are mainly localized over carbonyl group and phenyl ring are possible sites for electrophilic attack and the positive regions are localized at all the hydrogen atoms, indicating possible sites for nucleophilic attack. Local reactivity properties have been investigated using quantum chemical parameters and Fukui function analysis. The first and second-order hyperpolarizabilities were calculated. The calculated first order hyperpolarizability is commensurate with the documented worth of very similar derivatives and could be an interesting object for more experiment on nonlinear optics. The HOMO and LUMO energies also confirm that charge transfer occurs within the molecule. The NMR spectral assessment had been made choosing structure-property relationship by chemical shifts along with the magnetic shielding effects regarding the title compound. The magnetic susceptibility and thermodynamic property of the title compound for various temperatures also be discussed.

© 2017 Elixir All rights reserved.

Introduction

Acetophenones are compounds that exhibit interesting physiochemical and biological properties. They are found in nature [1, 2] and they can also be obtained by means of diverse synthesis procedure [3, 4]. Antibacterial activity can be mentioned among its biological properties. A recent study has linked the antibacterial activity of 20 acetophenones with their structural characteristics by using electronic and topological indices [5]. It has also been found that diazinium salts with dihydroxy acetophenone skeleton possess antimicrobial activity [6] and those complexes between p-substituted acetophenone and benzoyl hydrazone have antifungal activity [7]. On the other hand, substituted acetophenones are employed as synthesis reagents of several organic reactions. A well-known one is the condensation reaction in the alkaline medium of acetophenones and benzaldehydes in the synthesis of flavonoids (chalcones, flavones, and flavanones) [9, 10]. The complexation capacity of metallic ions exerted by flavonoids has been investigated in several reaction media and working condition. Acetophenone is one of the most typical aromatic carbonyls, which shows interesting photochemical properties [11, 12].

Halogen combined acetophenone like 4-chloro-2-bromoacetophenone possesses NLO properties [13]. NLO (non-linear optics) has wide applications in the field of telecommunication, optical mixing, electro-optic modulation, optical parametric oscillation, optical bistability, functioning as second harmonic generators, frequency converters and electro-optical modulators, etc., because of the large second order electric susceptibilities of organic materials. Since the second order electric susceptibility is related to the first hyperpolarizability, the search for organic chromophores with large first hyperpolarizability is fully justified. Because of these versatile behaviors of acetophenone derivatives, in the present study, FT-IR and FT-Raman spectra of NPE were reported both experimentally and theoretically.

The energies, degrees of hybridization, the population of the lone pairs of oxygen, nitrogen atoms, energies of their interaction with the antibonding orbital of the benzene ring and the electron density distributions and E(2) energies have been calculated by NBO analysis. The frontier molecular orbital, thermodynamic and magnetic properties of this title molecule have been extensively investigated.

Tele:

E-mail address: brsbala@rediffmail.com

© 2017 Elixir All rights reserved

2. Experimental details

The sample NPE in the solid form was procured from Lancaster Chemical Company, UK, it was used as such without further purification. The Fourier transform infrared (FT-IR) spectrum of the sample was recorded at room temperature in the region 4000-450 cm^{-1} using Perkin-Elmer spectrum1 spectrophotometer equipped with the composition of the pellet. The signals were collected for 100 scans with a scan interval of 1 cm^{-1} and at an optical resolution of 1.0 cm^{-1} . The Fourier transform Raman (FT-Raman) BRUKER-RFS 27 spectrometer was used for the FT-Raman spectral measurements at room temperature. The spectrometer consists of a quartz beam splitter and a high sensitive germanium diode detector cooled to the liquid nitrogen temperature. The sample was packed in a glass tube of about 5 mm diameter and excited in the 180° geometry with 1064 nm laser line at 100 MW power from a diode-pumped air cooled-cw Nd: YAG laser as an excitation wavelength in the region 5000-50 cm^{-1} . The signals were collected for 300 scans at the interval of 1 cm^{-1} and optical resolution of 2.0 cm^{-1} . NMR spectra (^1H and ^{13}C) for the title compound were recorded on a BRUKER Avance III 500 spectrometer at 500 MHz for ^1H and 75 MHz for ^{13}C , CDCl_3 as the solvent containing 0.03 vol.% TMS as an internal standard. The chemical shift values (ppm) and coupling constants (j) are given \square and Hz respectively.

3. Computational details

Calculations of the title compound were carried out with Gaussian09 program [14] using the DFT levels of theory using the standard B3LYP/ cc-pVDZ, B3LYP/cc-pVTZ basis sets to predict the molecular structure and vibrational wavenumbers. Molecular geometry (Fig. 1) was fully optimized by optimization algorithm using redundant internal coordinates. The computed wavenumber values contain known systematic errors and hence, we have used the scaling factors 0.9613 and 0.9747 for cc-pVDZ and cc-pVTZ basis sets, respectively [15]. The absence of imaginary wavenumbers of the calculated vibrational spectrum confirms that the structure deduced corresponds to minimum energy. The assignments of the calculated wavenumbers are aided by the animation option of GAUSSVIEW program, which gives a visual presentation of the vibrational modes [16].

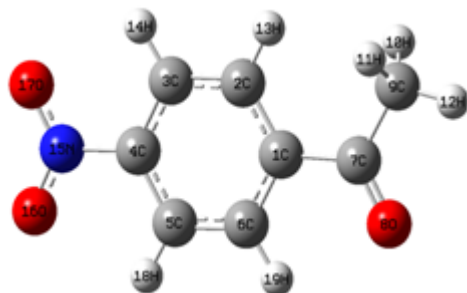


Fig.1 Optimized molecular structure of 1(4-Nitrophenyl)ethanone

The potential energy distribution (PED) is calculated with the help of MOLVIB program version 7.0 written by Sundius [17, 18].

3.1 Predictions of Raman intensities

The Raman activities (S_i) calculated with the help of GAUSSIAN 09 program were converted to relative Raman intensities (I_i) using the following relationship derived from the basic theory of Raman scattering [19-21].

$$I_i = f (\nu_0 - \nu_i)^4 S_i / \nu_i [1 - \exp(-hc\nu_i / kT)]$$

where ν_0 is the laser exciting frequency in cm^{-1} (in the present study, we have used the excitation wavenumber $\nu_0 = 9398.5 \text{ cm}^{-1}$ which corresponds to the wavelength of 1064 nm of a Nd: YAG laser), ν_i is the vibrational wavenumber of the i^{th} normal mode (in cm^{-1}) and S_i is the Raman scattering activity of the normal mode ν_i , f (is the constant equal to 10^{-12}) is the suitably chosen common normalization factor for all peak intensities, h , k , c and T are plank constant, Boltzmann constant, speed of light and temperature in Kelvin, respectively.

4. Result and discussions

The geometry of the molecule is possessing C_s point group symmetry. The 51 fundamental modes of vibrations are span into 35 in-plane modes of A' and 16 out-of-plane bending vibrations of A'' species. The observed and calculated FT-IR and FT-Raman spectra of NPE are shown in Fig. 2 and Fig. 3. The observed FT-IR and FT-Raman wavenumbers along with their relative intensities and probable assignments are summarized in Table 1.

4.1 Vibrational assignments

4.1.1 NO_2 modes

The calculated (scaled) wavenumbers, observed FT-IR, FT-Raman bands and assignment are given in Table 1. In the following discussion, the experimentally observed FT-IR (Fig.2) and FT-Raman (Fig.3) are compared with B3LYP/cc-pVTZ, cc-pVDZ values.

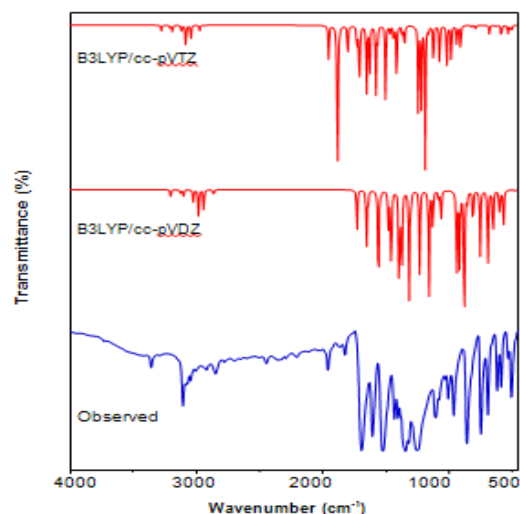


Fig.2 Observed FT-IR and simulated spectrum of 1(4-nitrophenyl)ethanone

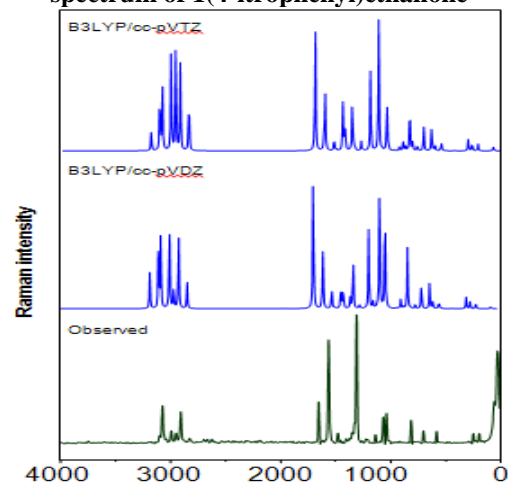


Fig.3 Observed FT-Raman and simulated spectrum of 1(4-Nitrophenyl)ethanone

Nitrobenzene derivative shows asymmetric NO₂ stretching mode in the region 1535±30 cm⁻¹ and symmetric NO₂ stretching modes in the region 1345±30 cm⁻¹ [22]. Raj et al. [23] reported NO₂ stretching modes at 1621, 1582, 1526, 1328 cm⁻¹ in FT-IR spectrum and at 1601, 1585, 1561, 1532, 1343, 1332 cm⁻¹ (theoretical) as NO₂ stretching modes. In the present study 1606vs (IR), 1610, 1605cm⁻¹ (DFT) are assigned to NO₂ asymmetric stretching mode. The observed and DFT calculation give 1343vs (IR), 1344vs (Raman), and 1349, 1345 (DFT) cm⁻¹ as symmetric stretching modes of NO₂ for the title compound. In aromatic compounds, the wagging modes of NO₂ is assigned at 740±50 cm⁻¹[22]. For the title compound, NO₂ wagging mode is reported at 745vs (IR), 745vs (Raman) and 752, 746 cm⁻¹ (DFT). The rocking mode of NO₂ is expected in the region 540±70 cm⁻¹[22] in aromatic nitro compounds. The deformation modes of NO₂ are reported at 744 (IR), 716, 821 cm⁻¹ (DFT) [24]. For the title compound, the bands at 529 cm⁻¹ in the IR spectrum are deformation modes of NO₂ and the calculated values are 531, 528 cm⁻¹.

4.1.2 C–N Modes

NO₂ group attached to phenyl ring by carbon atom C4 of NPE gives rise to three vibrational modes such as C–N stretching, C–N in-plane bending and C–N out-of-plane bending modes. The identification of C–N vibrations are very difficult task, since the mixing of several bands are possible in this region. The C–N stretching modes are expected in the range 1100 – 1300 cm⁻¹ [25]. The bands at 1103vs (IR), 1106, 1102 cm⁻¹ theoretically (B3LYP) are assigned as C–N stretching modes. Panicker et al. [26] reported the C–N stretching mode at 1215 cm⁻¹ theoretically. Sebastian and Sundaraganesan [27] reported the C–N stretching modes at 1122 and 1154 cm⁻¹ for the piperidine ring. The C–N in-plane bending vibration of a nitro group for the title compound assigned at 537(Raman), 540, 597(DFT) respectively. The C–N out-of-plane bending vibration for the title compound assigned at 55, 53(DFT) respectively.

4.1.3 C=O Modes

The wavenumber of the C=O stretch due to carbonyl group mainly depends on the bond strength, which in turn depends upon inductive, conjugative, steric effect and a lone pair of an electron on oxygen. The carbonyl stretching C=O vibration [22, 25, 28,] is expected in the region 1750-1680 cm⁻¹ and for the title compound, the C = O stretching modes are assigned at 1692 (IR), 1684 (Raman), 1688, 1684 cm⁻¹ (DFT) which are in agreement with reported literature. The in-plane and out-of-plane C=O deformations are expected in the region 625 ± 70 and 540 ± 80cm⁻¹, respectively [22]. The C=O deformation bands are observed at 616, 584 cm⁻¹ in the IR spectrum and 620, 615, 590, 585 cm⁻¹ theoretically (DFT). Gumus et al., [29] reported the C=O stretching modes at 1686, 1678, 1702 cm⁻¹ experimentally.

4.1.4 CH₃ Modes

The asymmetric and symmetric stretching vibrations of the methyl group in acetates are expected in the regions 2940- 3040 cm⁻¹ and 2910 -2903 cm⁻¹ [22]. Aromatic acetyl substituent absorbs in a narrow range 3000 – 3020 cm⁻¹, absorption sometimes coincides with the CH stretching mode of the ring [22]. For the title compound, methyl stretching vibrations are observed at 2920, 2845 cm⁻¹ in the IR spectrum, 2963, 2921, 2842 cm⁻¹ in the Raman spectrum and at 2966, 2965, 2924, 2920, 2845, 2843 cm⁻¹ theoretically (B3LYP/cc-pVDZ and cc-pVTZ).

The methyl asymmetric and symmetric deformations are expected in the region 1390 – 1480 and 1340 – 1390 cm⁻¹ [22]. The B3LYP calculations give 1435, 1433, 1416 and 1413 cm⁻¹ as asymmetric and symmetric deformation bands and the corresponding band in the IR spectrum is 1431cm⁻¹ and in the Raman spectrum are 1436, 1412 cm⁻¹(Table 1). According to Colthup et al.[28] in acetates the methyl next to C=O absorbs near 1374 cm⁻¹ due to symmetric deformation; the asymmetric methyl deformation absorbs weakly near 1430 cm⁻¹. The methyl rocking generally appears in the regions 1050 ± 30 and 975 ±45 cm⁻¹, as a weak, moderate or sometimes strong band, the wavenumber of which is coupled to the CC stretching vibrations [22], which occurs in the neighborhood of 900 cm⁻¹. The band at 1026 cm⁻¹ in IR spectrum, 1031, 1025, 1016, 1012 cm⁻¹ (DFT) was assigned as the rocking modes of the methyl group. The skeletal and other deformation bands of –C(=O)Me group and torsion modes are observed below 500 cm⁻¹. The methyl group torsion mode for the title compound is assigned at 192 cm⁻¹ in IR spectrum and theoretically (DFT) assigned at 196, 191cm⁻¹.

4.1.5 C–H, C–C modes

The phenyl ring CH stretching modes are assigned at 3107, 3006 cm⁻¹ in the IR spectrum (Fig.2), 3187, 3107, 3085, 3006 cm⁻¹ in the Raman spectrum (Fig.3) and at 3190, 3185, 3112, 3106, 3089, 3085, 3008, 3005 cm⁻¹ theoretically (B3LYP/cc-pVDZ & cc-pVTZ) as expected [22]. The CH in-plane and out-of-plane deformation modes of the phenyl ring are expected above and below 1000 cm⁻¹ [31]. For the title compound, these modes are assigned at 1402, 1245(IR), 1488, 1137 (Raman), 1493, 1488, 1410, 1405, 1250, 1244, 1140, 1135 cm⁻¹ (DFT) (in-plane) and 961, 856 (IR), 962, 855, 790 (Raman), 960, 913, 854, 789 cm⁻¹ (DFT) (out-of-plane) (Table 1).

For ortho-substituted benzene [22], the phenyl ring stretching modes are expected in the region 1620 – 1260 cm⁻¹. The phenyl ring stretching modes are observed at 1524, 1318 cm⁻¹ in IR spectrum (Fig. 2), 1595, 1512, 1175ms cm⁻¹ in the Raman spectrum (Fig.3). The DFT calculation gives these modes at 1598, 1594, 1515, 1514, 1325, 1318, 1181, 1174 cm⁻¹ as expected [22]. In ortho- substitution, the ring breathing mode has three wavenumber intervals depending on whether both substituents are heavy; or one of them is heavy, while the other is light; or both of them are light [30].In the first case, the interval in is 1100-1130 cm⁻¹; in thesecond case 1020-1070 cm⁻¹; while in the third case it is between 630 and 780 cm⁻¹ [30]. For the title compound PED analysis gives the ring breathing mode at 1087 cm⁻¹ (Table 1). The ring breathing mode of ortho-substituted benzene ring is reported at 1091cm⁻¹[22].

5. Geometrical parameters

The optimized geometrical (Fig.1) parameters (B3LYP/cc-pVDZ, B3LYP/cc-pVTZ) of 1(4-Nitrophenyl)ethanone are given in Table 2. The CC bond lengths in the phenyl ring lie between 1.3938-1.4099 (B3LYP) and here for the title compound, the benzene ring is a regular hexagon with bond lengths somewhere in between the normal values for a single (1.54 Å) and a double (1.33 Å) bond [32]. For the title compound, the C=O bond lengths are 1.22(DFT) which are in agreements with reported values [33-35].The calculated C–N distances is C4–N15 = 1.48, value indicates that the C–N bonds show single bond character in this fragment.

Table1.Experimental FT-IR, FT-Raman and Calculated DFT-B3LYP/cc-pVDZ, DFT-B3LYP/cc-pVTZ levels of vibrational frequencies (cm^{-1}), IR intensity (kmmol^{-1}) and Raman intensity (kmmol^{-1}) of 1(4-Nitrophenyl)ethanone.

No	Spe.	Observed frequencies (cm^{-1})		Calculated frequencies (cm^{-1})				IR Intensity (kmmol^{-1})		Raman Intensity (kmmol^{-1})		Vibrational assignments /PED ($\geq 10\%$)
		IR	Raman	B3LYP/cc-pVDZ		B3LYP/cc-pVTZ		B3LYP/ cc-pVDZ	B3LYP/ cc-pVTZ	B3LYP/ cc-pVDZ	B3LYP/ cc-pVTZ	
				Unscaled	Scaled	Unscaled	Scaled					
1	A'		3187vw	3238	3190	3228	3185	1.92	2.12	8.77	7.77	vCH(98)
2	A'	3107vs	3107w	3237	3112	3228	3106	1.27	1.08	5.86	4.44	vCH(98)
3	A'		3085w	3216	3089	3207	3085	2.22	2.58	3.74	3.01	vCH(97)
4	A'	3006vw	3006ms	3208	3008	3200	3005	3.62	2.94	4.87	3.84	vCH(98)
5	A'		2963w	3159	2966	3147	2965	7.74	9.09	9.49	7.79	v _{ass} CH ₃ (97)
6	A'	2920w	2921s	3106	2924	3091	2920	5.59	5.86	4.56	3.57	v _{ass} CH ₃ (98)
7	A'	2845w	2842vw	3038	2845	3036	2843	1.72	2.30	12.74	12.32	v _{ass} CH ₃ (98)
8	A'	1692vs	1684s	1777	1688	1761	1684	151.24	165.60	17.54	17.93	v CO(72)CC(21)
9	A'	1606vs		1671	1610	1647	1605	124.61	72.20	1.47	0.63	v _{ass} NO ₂ (66),vCC(21), δ CN(12)
10	A'		1595vs	1648	1598	1639	1594	3.73	5.72	89.23	84.55	vCC(78), δ CH(18)
11	A'	1524vs	1512ms	1618	1515	1589	1514	93.58	183.35	2.20	3.19	vCC(75),v _{ass} NO ₂ (16), δ CH(10)
12	A'		1488vw	1514	1493	1524	1488	0.84	0.30	0.29	0.24	δ CH(87),vCC(12)
13	A'	1431s	1436w	1450	1435	1481	1433	9.48	10.36	8.86	3.73	δ adCH ₃ (88)
14	A'		1412vw	1439	1416	1471	1413	9.21	10.41	3.35	1.98	δ adCH ₃ (86)
15	A'	1402s		1435	1410	1439	1405	19.50	17.96	2.57	1.66	δ CH(68),vCC(20), δ CC(10)
16	A'	1343vs	1344vs	1396	1349	1392	1345	264.15	27.39	100.00	1.95	v _{ss} NO ₂ (78),vCN(18)
17	A'	1318w		1380	1325	1375	1318	28.41	282.78	0.79	100.00	vCC(62), δ CH(21), δ CC(11)
18	A'		1260vw	1371	1266	1356	1261	64.32	28.08	1.83	0.63	δ sd(87)
19	A'	1245vs		1302	1250	1329	1244	3.09	5.73	0.27	0.15	δ CH(88)
20	A'		1175ms	1274	1181	1269	1174	203.68	228.81	18.65	15.50	vCC(68), δ sdCH ₃ (21)
21	A'		1137vw	1186	1340	1201	1135	6.55	3.05	2.20	1.57	δ CH(85)
22	A'	1103vs		1122	1106	1131	1102	28.73	6.66	35.74	0.15	vCN(75), δ CH(21)
23	A'	1077vw	1076s	1114	1075	1120	1075	11.56	24.96	0.57	34.74	δ CH(79)
24	A''	1026w		1089	1031	1093	1025	2.48	4.74	14.47	26.63	γ _{Ort} CH ₃ (68),vCC(19), δ _{Ring} (11)
25	A'			1045	1016	1053	1012	0.92	0.50	0.80	0.20	δ _{lpr} CH ₃ (81)
26	A'	1005s		1025	1009	1036	1004	8.52	9.65	0.32	0.28	δ _{Ring} (73), δ CH(16)
27	A''	961vs	962vw	1021	966	1025	960	0.20	0.06	0.26	0.10	γ CH(80), γ _{Ring} (11)
28	A''			998	916	1002	913	0.19	0.40	1.08	0.34	γ CH(78), γ _{Ring} (10)
29	A'			961	883	963	880	24.98	33.80	3.28	2.65	vCC(66), δ _{lpr} CH ₃ (20)
30	A''	856vs	855s	892	859	894	854	21.23	29.61	1.57	0.53	γ CH(75)
31	A'			871	822	872	819	51.58	52.15	18.56	18.52	δ _{Ring} (68)
32	A''		790vw	860	796	860	789	2.94	2.47	3.34	0.45	γ CH(77)
33	A''	745vs	745ms	770	752	776	746	10.74	17.57	2.83	1.99	γ _{Wagg} NO ₂ (76), γ CH(12), γ CN(11)
34	A''	690vs		757	693	759	690	18.12	16.26	10.69	9.22	γ _{Ring} (70), γ _{Wagg} NO ₂ (14), γ CH(11)
35	A'		627ms	712	631	713	625	22.86	19.69	0.49	0.02	δ _{Ring} (80)
36	A'	616vs		638	620	644	615	0.32	0.47	14.37	11.31	δ CO(66), δ CC(21)

37	A''	584vs		621	590	622	585	14.68	16.21	3.76	4.23	γ CO(58), γ CH(21)
38	A'		537vw	599	540	597	537	6.00	8.20	1.35	0.69	δ CN(78), δ CC(18)
39	A'	529w		542	531	541	528	1.71	1.39	4.58	4.15	δ_{Rock} NO ₂ (76), δ CO(18)
40	A''	503vs		510	506	508	501	11.51	9.78	0.22	0.32	γ_{Ring} (66), γ CO(16)
41	A'			456	410	453	406	0.36	0.67	0.57	0.28	δ CC(75)
42	A''			435	371	436	367	2.14	1.99	0.02	0.05	γ_{Ring} (79)
43	A'		297ms	423	301	421	296	0.00	0.00	0.01	0.01	Ring breathing(75)
44	A'		281vw	295	285	295	280	0.05	0.05	20.88	15.96	δ CC(63), δ CN(20)
45	A''		245ms	275	249	275	244	3.19	3.42	14.65	11.10	γ CC(68), γ CN(21)
46	A''		192vw	244	196	241	191	0.83	0.70	15.33	11.45	τ CH ₃ (71)
47	A'			178	142	161	136	0.25	5.12	0.08	0.41	δ COCH ₃ (61), δ_{rock} (18)
48	A''		110w	161	112	159	110	4.79	0.10	0.53	0.09	γ COCH ₃ (60)
49	A''		78s	82	79	80	78	4.43	3.57	6.36	0.01	γ CC(69), γ CN(21)
50	A''			77	55	64	53	0.31	1.85	57.31	45.84	γ CN(60), γ CO(29), γ_{Ring} (10)
51	A''			50	43	42	40	1.43	1.77	11.34	12.96	τ NO ₂ (61)

v-stretching, δ -in-plane bending, γ -out-of-plane bending, ρ -scissoring, σ -rocking, τ -twisting, δ ring-in-plane bending ring, γ ring-out-of -plane bending ring .

Also the C–N bond distances were found to be equal with the average value for a single C–N bond (1.47Å), but significant longer than a C=N double bond (1.22Å) [36], suggesting some multiple bond character is present. The C=C bond length is 1.34 and the C–C bond lengths lie in the range 1.39–1.52 Å which are in agreement with experimental reported values [37]. At C1 position, the bond angles are C2–C1–C6 = 119.37°, C2–C1–C7 = 122.81°, C6–C1–C7 = 117.82°, and this asymmetry shows the interaction between C7=O8 with the H19. Similarly at C4 position, the bond angles C3–C4–N15 is reduced by 1.20°, C3–C4–C5 is increased by 2.23° and C5–C4–N15 is decreased by 1.03° which shows the interaction between the phenyl ring and NO₂ group. In the case of NPE, the orientations of the carbonyl, methyl and nitro groups with respect to the aromatic ring are perfectly planar. This is confirmed by experimental reported values [37] and DFT level theoretical studied dihedral angles, C6–C1–C7–C9 = 180°; C6–C1–C7–O8 = 0°; C2–C1–C7–O8 = 180°; C7–C1–C2–C3 = 180°; C7–C1–C6–C5 = 180°; C3–C4–N15–O16 = –180°; C5–C4–N15–O17 = –180°; N15–C4–C5–C6 = 180° and so on.

6. NMR spectra

The absolute isotropic chemical shielding of the title compound was calculated by B3LYP/ GIAO model [38] and relative chemical shift was then estimated by using the corresponding TMS shielding: $\sigma_{\text{calc}}(\text{TMS})$ is calculated in advance at the same theoretical level. Numerical values of chemical shift $\delta_{\text{calc}} = \sigma_{\text{calc}}(\text{TMS}) - \sigma_{\text{calc}}$ together with calculated values $\sigma_{\text{calc}}(\text{TMS})$, are in given Table 3. The experimental values are: ¹H; 2.497, 6.646, 6.630, 7.789, 7.806. It could be seen from Table 3 that chemical shift was in agreement with the experimental ¹H–NMR data.

Thus, the results showed that the predicted proton chemical shifts were in good agreement with the experimental data for the title compound. The experimental ¹H and ¹³C NMR chemical shifts are represented in the Fig.4. The protons of the phenyl rings resonate in the range 7.809–6.630 ppm experimentally. The circulation of the double bond electrons generates a secondary magnetic field that accounts for the formation of magnetic anisotropy. Therefore, chemical shifts of the hydrogen atoms of the anhydride group are observed at 7.809, 7.789, 6.646 and 6.630 ppm. Due to the electron withdrawing C=O group, decrease the shielding of the neighboring hydrogen atoms and hence chemical shifts obtained and calculated for these hydrogen atoms are low.

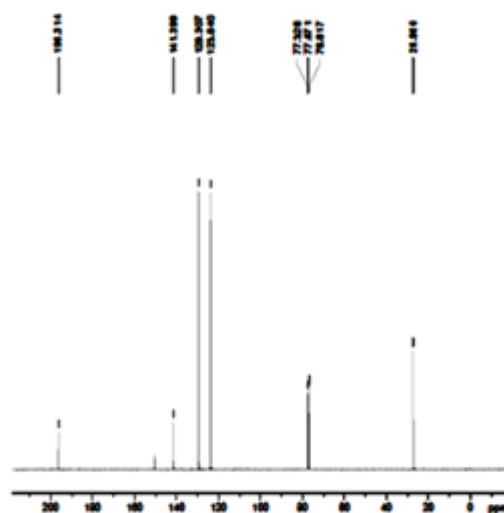
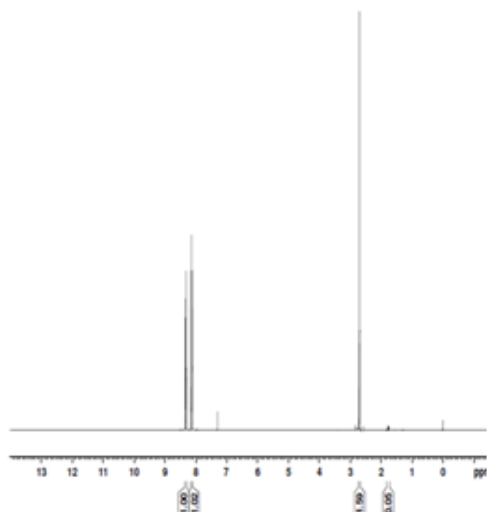


Fig. 4 ¹³C and ¹H NMR spectra of 1(4-Nitrophenyl)ethanone

Looking at the predicted and measured δ values for ¹³C NMR spectrum, the biggest difference can be observed for the carboxyl carbon 196 ppm (C7), followed by the nitro-substituted ring carbon 151 ppm (C4). From the measured spectrum, we have assigned the δ values 196, 151, 130, 127, 113, 26 ppm for C7, C4, C1, C2, C6, C3, C5 and C9 respectively.

7. Molecular electrostatic potential

The molecular electrostatic potential (MEP) is a well-established method to give the reactive properties of a wide variety of chemical systems in both electrophilic and nucleophilic reaction, the study of biological recognition processes and hydrogen bonding interaction [39, 40]. To predict the reactive regions for electrophilic and nucleophilic attack for the investigated molecule, the MEP at the DFT optimized geometry was calculated, the minimum and maximum limits of the electrostatic potential observed in NPE are $\pm 4.036 e^{-2}$. The different values of the electrostatic potential at the surface are represented by different colors (Fig.5) and potential increases in the order red < orange < yellow < green < blue. The negative (red, orange and yellow) regions of the MEP are related to electrophilic reactivity. The maximum negative region is localized over the carbonyl group oxygen and nitrogen atoms and the maximum positive region is localized on hydrogen atoms indicating a possible site for nucleophilic attack. These sites give information about the region from which the compound can have intermolecular interactions. This predicted site shows the most reactive site for both electrophilic and nucleophilic attack.

8. First hyperpolarizability

Nonlinear optics deals with the interaction of applied electromagnetic fields in various materials to generate new electromagnetic fields, altered in wavenumber, phase or other physical properties [41]. Organic molecules able to manipulate photonic signals efficiency are of importance in technologies such as optical communication, optical computing, and dynamic image processing [42, 43]. In this context, the first hyperpolarizability of the title compound is calculated in the present study. The first hyperpolarizability (β_0) of the title compound is calculated using DFT method, based on the finite field approach.

Table 2. Optimized structural parameters of 1(4-Nitrophenyl)ethanone utilizing B3LYP/cc-pVDZ and B3LYP/cc-pVTZ density functional calculation.

Parameters	Bond length Value(Å)			Parameters	Bond angle Value(Å)			Parameters	Dihedral angle (Å)		
	B3LYP/ cc-pVDZ	B3LYP/ cc-pVTZ	Exp*.		B3LYP/ cc-pVDZ	B3LYP/ cc-pVTZ	Exp.		B3LYP/ cc-pVDZ	B3LYP/ cc-pVTZ	Exp*.
C1-C2	1.41	1.40	1.392	C2-C1-C6	119.37	119.30	120.2	C6-C1-C2-C3	0.00	0.00	
C1-C6	1.41	1.40	1.403	C2-C1-C7	122.81	122.54	123.0	C6-C1-C2-H13	180.00	180.00	
C1-C7	1.51	1.50	1.496	C6-C1-C7	117.82	118.16	116.8	C7-C1-C2-C3	180.00	180.00	178.6
C2-C3	1.40	1.39	1.390	C1-C2-C3	120.57	120.65	120.1	C7-C1-C2-H13	0.00	0.00	
C2-H13	1.09	1.08	0.950	C1-C2-H13	120.61	120.52	120.0	C2-C1-C6-C5	0.00	0.00	0.7
C3-C4	1.39	1.39	1.365	C3-C2-H13	118.82	118.83	119.7	C2-C1-C6-H19	-180.00	-180.00	
C3-H14	1.09	1.08	0.950	C2-C3-C4	118.58	118.58	120.6	C7-C1-C6-C5	-180.00	-180.00	179.1
C4-C5	1.40	1.39	1.392	C2-C3-H14	122.05	121.78		C7-C1-C6-H19	0.00	0.00	
C4-N15	1.48	1.48	1.478	C4-C3-H14	119.37	119.65	119.7	C2-C1-C7-O8	180.03	180.01	179.3
C5-C6	1.39	1.38	1.377	C3-C4-C5	122.23	122.17		C2-C1-C7-C9	0.01	0.01	-1.5
C5-H18	1.09	1.08		C3-C4-N15	118.80	118.84	118.2	C6-C1-C7-O8	0.03	0.01	0.9
C6-H19	1.09	1.08	0.950	C5-C4-N15	118.97	118.99	119.3	C6-C1-C7-C9	180.01	180.01	179.9
C7-O8	1.22	1.21	1.213	C4-C5-C6	118.51	118.57	117.5	C1-C2-C3-C4	0.00	0.00	-0.3
C7-C9	1.52	1.51	1.515	C4-C5-H18	119.39	119.63	121.3	C1-C2-C3-H14	-180.00	-180.00	
C9-H10	1.10	1.09		C6-C5-H18	122.10	121.80	121.3	H13-C2-C3-C4	-180.00	-180.00	
C9-H11	1.10	1.09		C1-C6-C5	120.74	120.73		H13-C2-C3-H14	0.00	0.00	
C9-H12	1.10	1.09		C1-C6-H19	118.21	118.42		C2-C3-C4-C5	0.00	0.00	0.5
N15-O16	1.22	1.22	1.215	C5-C6-H19	121.06	120.85		C2-C3-C4-N15	-180.00	-180.00	
N15-O17	1.22	1.22	1.224	C1-C7-O8	119.91	120.08	121.0	H14-C3-C4-C5	180.00	180.00	
				C1-C7-C9	118.88	118.93	116.4	H14-C3-C4-N15	0.00	0.00	
				O8-C7-C9	121.21	120.99	122.6	C3-C4-C5-C6	0.00	0.00	-0.1
				C7-C9-H11	110.88	110.96		N15-C4-C5-C6	180.00	180.00	179.8
				C7-C9-H12	108.82	108.73		C3-C4-N15-O16	-180.00	-180.00	174.7
				H10-C9-H11	107.30	107.34		C5-C4-N15-O17	-180.01	-180.01	175.7
				H10-C9-H12	109.47	109.41		C1-C7-C9-H10	-59.53	-59.62	
				H11-C9-H12	109.47	109.41		C1-C7-C9-H11	59.56	59.63	
				C4-N15-O16	117.38	117.52	118.0	O8-C7-C9-H10	120.45	120.38	
				C4-N15-O17	117.42	117.55	118.0	O8-C7-C9-H11	-120.46	-120.37	

*Taken from Ref. [37]

Table 3. NMR Chemical shielding anisotropy (CSA) parameters of 1(4-Nitrophenyl)ethanone.

Proton	σ_{Tms}	B3LYP/ pVDZ σ_{calc}	cc- δ_{calc} ($\sigma_{Tms} - \sigma_{calc}$)	Exp δ_{ppm}	Carbo n	σ_{Tms}	B3LYP / cc-VDZ σ_{calc}	δ_{calc} ($\sigma_{Tms} - \sigma_{calc}$)	Exp δ_{ppm}
H10	31.8821	29.47	2.4121	2.497	C7	182.46		194.80	196
H11	31.8821	29.47	2.4121	2.497	C4	182.46	31	151.46	151
H12	31.8821	29.35	2.5321	2.497	C1	182.46	52	130.46	130
H13	31.8821	23.76	8.1221	7.809	C2	182.46	54	128.46	127
H19	31.8821	23.64	8.2421	7.789	C6	182.46	55	127.46	127
H14	31.8821	25.68	6.2021	6.646	C3	182.46	69	113.46	113
H18	31.8821	25.62	6.2621	6.630	C5	182.46	69	113.46	113
					C9	182.46	155.84	26.62	26

In the presence of an applied electric field, the energy of a system is a function of the electric field, first, hyperpolarizability is a third rank tensor that can be described by a $3 \times 3 \times 3$ matrix. The 27 components of the 3D matrix can be reduced to 10 components due to the Kleinman symmetry [44]. When the electric field is weak and homogeneous, this expansion becomes

$$E = E_0 - \sum_x \mu_x F^x - \frac{1}{2} \sum_{xy} \alpha_{xy} F^x F^y - \frac{1}{6} \sum_{xyz} \beta_{xyz} F^x F^y F^z - \frac{1}{24} \sum_{xyzw} \gamma_{xyzw} F^x F^y F^z F^w + \dots$$

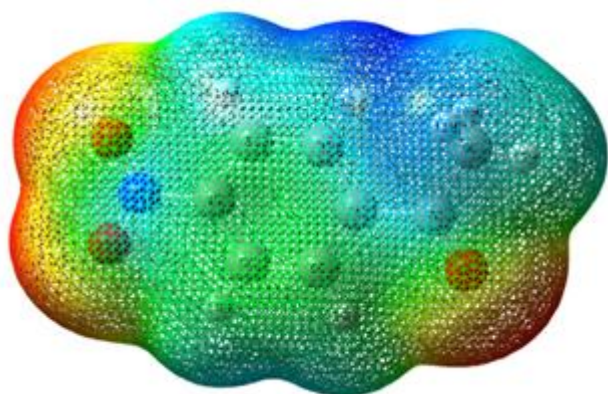


Fig 5. Molecular electrostatic potential plot of 1(4-Nitrophenyl)ethanone.

where E_0 is the energy of the unperturbed molecule, F^x is the field at the origin, μ_x , α_{xy} , β_{xyz} and γ_{xyzw} are the components of dipole moment, polarizabilities, the first hyperpolarizabilities and second hyperpolarizabilities, respectively. For the title compound, the dipole moment, linear polarizability and first hyperpolarizability were obtained from theoretical calculations are listed in Table 4. The calculated first hyperpolarizability of the title compound is 2.7301×10^{-30} esu which is 21 times that of standard NLO material urea (0.13×10^{-30} esu) [45]. The reported values of hyperpolarizability of similar derivatives are 2.24×10^{-30} and 2.39×10^{-30} esu [46, 47]. We conclude that the NPE is an attractive object for future studies of nonlinear optical properties.

9. Natural bond orbital analysis

The natural bond orbitals (NBO) calculations were performed using NBO 3.1 program [48] as implemented in the Gaussian09 [14] package at the DFT/B3LYP level and the important interactions are given in Table 5. NBO analysis provides an accurate method for studying interaction and gives an efficient basis for investigating charge transfer or hyper-conjugative interactions in molecular systems. A large value of second order stabilization energy $E(2)$ shows that the interaction is more intense between electron donors and acceptors. The delocalization of electron density between occupied Lewis type NBO orbital and formally unoccupied non-Lewis orbital correspond to a stabilizing donor-acceptor interaction. In order to characterize the intra and intermolecular interactions quantitatively, a second order perturbation theory is applied that gives the energy lowering associated with such interactions. For each donor and acceptor, the strength of various types of interactions or stabilization energy $E(2)$ associated with electron delocalization between donor and acceptor is estimated by the second order energy lowering equation [49, 50] as

$$E(2) = E_{ij} = q_i (F_{ij})^2 / (E_j - E_i)$$

Where q_i is the donor orbital occupancy, E_i and E_j are the diagonal elements and F_{ij} is the off-diagonal NBO Fock matrix element.

In NBO analysis, large $E(2)$ values shows the intensive interaction between electron donors and electron acceptors and greater the extent of the whole system, the possible intensive interactions are given in Table 5. The important intra-molecular hyper-conjugative interactions are C4-N15 from O_8 of $lp(O_8) \rightarrow \sigma^*$ (C4-N15), from O_{16} of $lp(O_{16}) \rightarrow \sigma^*$ (C4-N15), N15-O16 from O_{17} of $lp(O_{17}) \rightarrow \sigma^*$ (N15-O16), C2-C3 from n of σ (C2-C3) $\rightarrow \sigma^*$ (C4-N15), C4-C5 from ln of σ (C4-C5) $\rightarrow \sigma^*$ (C3-C4) with stabilization energies, 4.63, 4.67, 2.1, 4.83 and 4.676 kJ/mol respectively. The accumulation of natural charges and electron population of atoms in core, valance, Rydberg orbital of the title compound is presented in Table 6. The NBO analysis also describes the bonding in terms of the natural hybrid orbital with higher and lower energy orbitals. Table 7. depicts the bonding concepts such as type of bond orbital, their occupancies, the natural atomic hybrids of which the NBO is occupancies, giving the percentage of the NBO on each hybrid, the atom label and a hybrids label showing the hybrid orbital (sp_x) composition (the amount of s-character, p-character, etc.) of 1(4-Nitrophenyl)ethanone determined by DFT/B3LYP method with cc-pVDZ and cc-pVTZ basis sets. The occupancies of NBO'S reflecting their exquisite dependence on the chemical environment. The Lewis structure that is closet to the optimized structure is determined. For example, the bonding orbital for C1-C2 with 1.9747 electrons has 50.63% C1 character in a $sp^{1.85}$ hybrid and has 49.37% C2 character in a $sp^{1.84}$ hybrid orbital.

In case of the bonding orbital for C4-N15 with 1.9890 electrons has 37.26% C4 character in a $sp^{3.07}$ hybrid and has 62.74% N15 character in a $sp^{1.76}$ hybrid orbital and the bonding orbital for C7-O8 with 1.9962 electrons has 33.05% C7 character in a $sp^{2.27}$ hybrid and has 66.95% O8 character in a $sp^{1.32}$ hybrid orbital and so on. The C-C bonds of the aromatic ring possess more p character than s character. This is clearly indicates that the delocalization of p electrons among all the carbon atoms.

10. Frontier molecular orbital analysis

To explain several types of reactions and for predicting the most reactive position in conjugated systems, molecular orbital and their properties such as energy are used [51,52]. The HOMO and LUMO energy values and their energy gap value reflect the biological activity of the molecule. A molecule having a small frontier orbital gap is more polarizable and is generally associated with a high chemical reactivity and low kinetic stability [53-55]. The plot of highest occupied molecular orbital (HOMO) and the lowest unoccupied molecular orbital (LUMO) of the title compound are shown in Fig.6. In the title compound, the HOMO of π nature is delocalized over the rings and the oxygen atom O_8 whereas the LUMO is located over the complete molecule except methyl group. The HOMO-LUMO energy gap of the title molecule calculated by B3LYP/cc-pVDZ method is -4.4161 eV. For understanding various aspects of pharmacological sciences including drug design and the possible eco-toxicological characteristics of the drug molecules, several new chemical reactivity descriptors have been proposed. Using HOMO and LUMO orbital energies, the ionization energy and electron affinity can be expressed as $I = -E_{HOMO}$, $A = -E_{LUMO}$ [56]. The hardness $\eta = (I-A)/2$ and $\mu = -(I+A)/2$, where I and A are the first ionization potential, and electron affinity of the chemical species [57].

TTable 4. Significant second-order interaction energy (E (2), kcal/mol) between donor and acceptor orbital of 1(4- nitrophenyl) ethanone calculated at B3LYP/cc-pVDZ level of theory.

Donor (i)	Acceptor (j)		E(2) ^a kcal/mol	($\epsilon_i - \epsilon_j$) ^b a.u	F_{ij} ^c a.u	or (i)	Acceptor (j)		E(2) ^a kcal/mol	($\epsilon_i - \epsilon_j$) ^b a.u	F_{ij} ^c a.u	
σ (C1- C2)	σ^* (C1 - C6)	1.9747	4.09	1.3	0.065	σ (C4- N15)	σ^* (C1 - C6)	1.9890	3.05	1.29	0.056	
	σ^* (C2 - C3)		2.97	1.29	0.055		σ (C5- C6)	σ^* (C1 - C7)	1.9734	3.81	1	0.059
	σ^* (C3 - H14)		2.38	1.2	0.048			σ^* (C4 - C5)		3.08	1.27	0.056
σ (C1- C6)	σ^* (C6 - H19)		2.43	1.2	0.048		σ^* (C4 - N15)		4.93	0.99	0.064	
	σ^* (C1 - C2)	1.9740	4.13	1.29	0.065		σ^* (C1 - C6)		4.12	1.12	0.061	
	σ^* (C2 - H13)		2.73	1.18	0.051	σ (C5- H18)	σ^* (C3 - C4)	1.9772	4.84	1.1	0.065	
	σ^* (C5 - C6)		2.57	1.29	0.051		σ^* (C1 - C2)		4.96	1.11	0.066	
σ (C1- C7)	σ^* (C5 - H18)		2.42	1.2	0.048	σ (C6- H19)	σ^* (C4 - C5)	1.9785	4.23	1.1	0.061	
	σ^* (C2 - C3)	1.9776	2.79	1.22	0.052	σ (C7- O8)	σ^* (C1 - C6)	1.9962	2.68	1.21	0.051	
	σ^* (C5 - C6)		2.83	1.22	0.052	σ (C7- C9)	σ^* (C7 - O8)	1.9887	1.91	1.09	0.041	
σ (C2- C3)	σ^* (C1 - C2)	1.9732	3.4	1.29	0.059	σ (C9- H10)	σ^* (C7 - O8)	1.9734	4.4	0.53	0.044	
	σ^* (C1 - C7)		3.84	1.11	0.059	σ (C9- H11)	σ^* (C7 - O8)	1.9734	4.4	0.53	0.044	
	σ^* (C3 - C4)		3.09	1.28	0.056		σ^* (C1 - C7)		3.91	0.91	0.054	
	σ^* (C4 - N15)		4.83	1	0.063	lp (O8)	σ^* (C4 - N15)	1.9742	4.67	1.07	0.065	
σ (C2- H13)	σ^* (C1 - C6)	1.9785	4.66	1.13	0.065	lp (O16)	σ^* (C4 - N15)	1.9794	4.67	1.07	0.065	
	σ^* (C3 - C4)		4.05	1.11	0.06	lp (O17)	σ^* (N15 - O16)	1.9794	2.1	1.27	0.046	
	σ^* (C2 - C3)	1.9752	2.65	1.31	0.053							
σ (C3- C4)	σ^* (C2 - H13)		2.49	1.2	0.049							
	σ^* (C4 - C5)		4.61	1.29	0.069							
	σ^* (C1 - C2)	1.9774	4.22	1.12	0.061							
σ (C3- H14)	σ^* (C4 - C5)		4.8	1.1	0.065							
	σ^* (C3 - C4)	1.9753	4.67	1.29	0.069							
σ (C4- C5)	σ^* (C5 - C6)		2.53	1.3	0.051							

^aE(2) means energy hyper conjugative interactions. ^bEnergy difference between donor and acceptor i and j NBO orbitals.

^cF(i,j) is the Fock matrix element between i and j NBO orbitals.

Table5.Accumulation of natural charges and electron population of atoms in core, valance, Rydberg orbitals of 1(4-Nitrophenyl)ethanone

Atoms ^a	Charge (e)	Natural population (e)			Total (e)	Atoms ^b	Charge(e)	Natural population (e)			Total (e)
		Core	Valence	Rydberg				Core	Valence	Rydberg	
C4	0.074	1.999	3.903	0.024	5.926	C1	-0.125	1.999	4.109	0.017	6.125
C7	0.594	1.999	3.362	0.045	5.406	C2	-0.199	1.999	4.187	0.013	6.199
H10	0.233	0.000	0.764	0.003	0.767	C3	-0.194	1.999	4.179	0.017	6.194
H11	0.233	0.000	0.764	0.003	0.767	C5	-0.194	1.999	4.177	0.018	6.194
H12	0.244	0.000	0.753	0.004	0.756	C6	-0.173	1.999	4.158	0.017	6.173
H13	0.235	0.000	0.762	0.003	0.765	O8	-0.539	2.000	6.531	0.009	8.539
H14	0.255	0.000	0.741	0.004	0.745	C9	-0.717	1.999	4.710	0.008	6.717
N 15	0.522	1.999	4.419	0.059	6.478	O 16	-0.376	2.000	6.362	0.014	8.376
H18	0.256	0.000	0.740	0.004	0.744	O 17	-0.378	2.000	6.364	0.014	8.378
H19	0.249	0.000	0.746	0.005	0.751						

^a Atoms containing positive charges ^b Atoms containing negative charges

Table6. Natural atomic orbital occupancies and energies of most interacting NBO's of 1(4- Nitrophenyl)ethanone along with their hybrid atomic orbitals and hybrid directionality.

Parameters ^a (A-B)	Occupancies	ED _A %	ED _B %	ED/e(a.u) (A,B)	Hybrid	AO(%) ^b
σ(C1 - C2)	1.9747	50.63	49.37	0.7027, 0.7115	sp ^{1.85} (C1) sp ^{1.84} (C2)	(35.13%)(64.84%)+(35.17%)(64.79%)
π(C1 -C 2)	1.6260	50.62	49.38	0.7115 0.7027	sp ^{1.00} (C1) sp ^{1.00} (C2)	(0.00%)(99.96%)+(0.00%)(99.95%)
σ(C1 - C6)	1.9740	51.02	48.98	0.71430.6998	sp ^{1.83} (C1) sp ^{1.84} (C6)	(35.29%)(64.68%)+(35.20%)(64.76%)
σ(C1 - C7)	1.9776	53.06	46.94	0.72840.6851	sp ^{2.38} (C1) sp ^{1.89} (C7)	(29.55%)(70.41%)+(34.55%)(65.39%)
σ(C2 - C3)	1.9732	49.94	50.06	0.7067,0.7075	sp ^{1.83} (C2) sp ^{1.78} (C3)	(35.26%)(64.70%)+(35.93%)(64.04%)
σ(C2 -H13)	1.9785	61.86	38.14	0.7865,0.6176	sp ^{2.39} (C2) sp ^{0.00} (H13)	(29.46%)(70.52%)+(99.90%)(0.10%)
σ(C3 - C4)	1.9752	49.08	50.92	0.7006, 0.7136	sp ^{1.88} (C3) sp ^{1.66} (C4)	(34.65%)(65.31%)+(37.62%)(62.35%)
π(C3 - C4)	1.6422	46.13	53.87	0.6792, 0.7340	sp ^{1.00} (C4) sp ^{1.00} (C3)	(0.00%)(99.93%)+(0.00%)(99.97%)
σ(C3 H14)	1.9774	62.92	37.08	0.7932,0.6089	sp ^{2.41} (C3) sp ^{0.00} (H14)	(29.33%)(70.66%)+(99.89%)(0.11%)
σ(C4 - C5)	1.9753	51.06	48.94	0.7145, 0.6996	sp ^{1.65} (C4) sp ^{1.89} (C5)	(37.68%)(62.31%)+(34.55%)(65.34%)
σ(C4 -N15)	1.9890	37.26	62.74	0.6104,0.7921	sp ^{3.07} (C4) sp ^{1.76} (N15)	(24.53%)(75.34%)+(36.23%)(63.74%)
σ(C5 - C6)	1.9734	50.31	49.69	0.7093, 0.7049	sp ^{1.78} (C5) sp ^{1.86} (C6)	(35.88%)(64.03%)+(34.94%)(65.04%)
π(C5 - C6)	1.6287	50.20	49.80	0.7085, 0.7057	sp ^{1.00} (C5) sp ^{1.00} (C6)	(0.00%)(99.92%)+(0.00%)(99.96%)
σ(C5 -H18)	1.9772	62.99	37.01	0.7936,0.6084	sp ^{2.41} (C5) sp ^{0.00} (H18)	(29.35%)(70.60%)+(99.92%)(0.08%)
σ(C6 -H19)	1.9785	62.72	37.28	0.7920, 0.6105	sp ^{2.36} (C6) sp ^{0.00} (H19)	(29.77%)(70.21%) + (99.89%)(0.11%)
σ(C7 - O8)	1.9962	33.05	66.95%	0.5749, 0.8182	sp ^{2.27} (C7) sp ^{1.32} (O8)	(30.48%)(69.31%)+(43.10%)(56.81%)
π(C7 -O8)	1.9719	33.96	66.04%	0.5827, 0.8127	sp ^{1.00} (C7) sp ^{1.00} (O8)	(0.00%)(99.57%) + (0.00%)(99.86%)
σ(C7 - C9)	1.9887	48.69	51.31%	0.6978,0.7163	sp ^{1.87} (C7) sp ^{2.76} (C9)	(34.78%)(65.17%)+(26.56%)(73.39%)
σ(C9 -H10)	1.9734	61.40	38.60%	0.7836, 0.6213	sp ^{3.13} (C9) sp ^{0.00} (H10)	(24.18%)(75.79%)+(99.90%)(0.10%)
σ(C9 -H11)	1.9734	61.40	38.60%	0.7836,0.6213	sp ^{3.13} (C9) sp ^{0.00} (H11)	(24.18%)(75.79%)+(99.90%)(0.10%)
σ(C9 -H12)	1.9875	62.23	37.77%	0.7889, 0.6146	sp ^{3.00} (C9) sp ^{0.00} (H12)	(25.01%)(74.97%)+(99.90%)(0.10%)
σ(N 15 -O16)	1.9948	47.93	52.07%	0.6923,0.7216	sp ^{2.15} (N15) sp ^{2.61} (O16)	(31.72%)(68.16%) +(27.63%)(72.21%)
π(N15 -O16)	1.9852	40.45	59.55%	0.6360,0.7717	sp ^{1.00} (N15) sp ^{1.00} (O16)	(0.00%)(99.68%)(0.00%)(99.81%)
σ(N15-O17)	1.9948	47.92	52.08%	0.6922,0.7217	sp ^{2.15} (N15) sp ^{2.6} (O17)	(31.71%)(68.16%)+(27.65%)(72.19%)
σ(O8)	1.9742	-	-	-	sp ^{0.76}	(56.89%)(43.09%)
π(O8)	1.8838	-	-	-	sp ^{1.00}	(0.00%)(99.92%)
σ(O16)	1.9794	-	-	-	sp ^{0.38}	(72.44%)(27.55%)
π(O16)	1.8923	-	-	-	sp ^{1.00}	(0.00%)(99.92%)
σ(O17)	1.9794	-	-	-	sp ^{0.38}	(72.42%)(27.57%)
π(O17)	1.8925	-	-	-	sp ^{1.00}	(0.00%)(99.92%)
π (O17)	1.4340	-	-	-	sp ^{1.00}	(0.00%)(99.84%)

^a For numbering of atoms refer Fig. 1. ^b Percentage of s-type and p-type sub shell of an atomic orbitals are given in their respective brackets

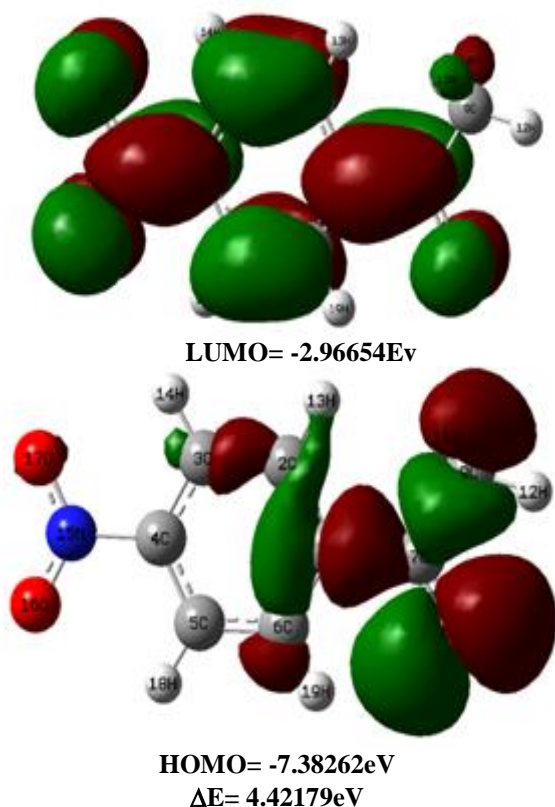


Fig.6 HOMO-LUMO Plot of 1(4-Nitrophenyl)ethane

For the title compound, the quantum chemical parameters are calculated and presented in Table 8, which are $E_{\text{HOMO}} = -7.3826$ eV, $E_{\text{LUMO}} = -2.9665$ eV, energy gap = $E_{\text{HOMO}} - E_{\text{LUMO}} = -4.4161$ eV, Ionization potential (I) = 7.3826 eV, Electron affinity (A) = 2.9665 eV, global hardness (η) = 2.2080 eV, chemical potential (μ) = -5.1746 eV, global electrophilicity (ω) = $\mu^2/2\eta = 6.0634$ eV. It is seen that the chemical potential of the title compound is negative and it means that the compound is stable.

11. Magnetic susceptibility

Magnetic susceptibility results from the response of electronic orbits and/or unpaired spins to an applied field. In paramagnetic materials χ is positive that is, for which M is parallel to B. The susceptibility is very small: 10^{-4} to 10^{-5} . The fact that these compounds have incomplete atomic shells is what is responsible for their paramagnetic behavior. They all have a critical below which the variation of susceptibility with temperature is very different from its variation above this temperature. A paramagnetic compound will have some electrons with unpaired spins. Paramagnetism derives from the spin and orbital angular moment of electrons. This type of magnetism occurs only in compounds containing unpaired electrons, as the spin and orbital angular momenta is cancelled out when the electrons exist in pairs. A plot of χ vs $1/\text{temperature}$ is known as a Curie plot. Ideally, it should be linear if the Curie-Weiss law is obeyed. For the title compound the plot of χ vs $1/T$ is linear hence Curie-Weiss law is obeyed. From such a plot, we can then extract the Curie constant from the slope and the Weiss constant from the x-Intercept [58]. For NPE, Table 9 shows the variation of susceptibility with temperature and Fig.7 shows the Curie pilot. The plot shows that NPE is paramagnetic in nature. The following linear equation (regression equation) is considered to be the best fit to predict the value of Curie constant. $Y=4447x+8E-05$ (R2-1)

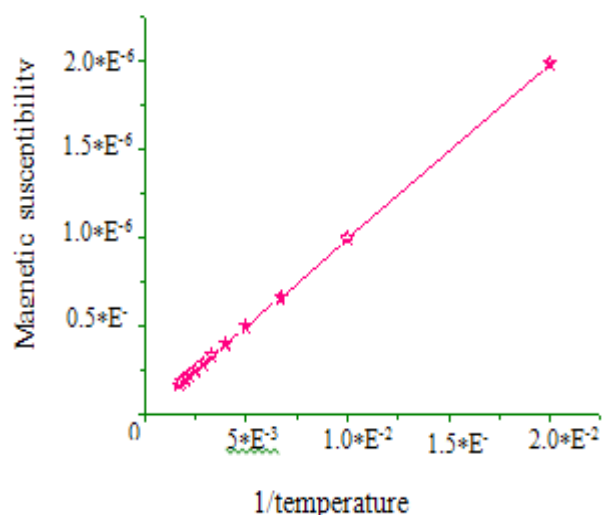


Fig7. Magnetic property plot of 1(4-nitrophenyl)ethane.

Curie constant = 0.00027, Weiss constant = 5.12379×10^{-7} (BM). The Weiss constant is almost zero. Hence the plot passes through the origin which proves the paramagnetic nature of NPE.

12. Mulliken atomic charges

Millikan [59] atomic charge calculation has an important role for the application of quantum chemical calculations (QCC) of the molecular system. Atomic charge affects dipole moment, polarizability, electronic structure and other molecular properties of the system.

The calculated Mulliken charge (e) values of NPE are listed in Table 10. It is clearly shown that the carbon atoms attached to hydrogen atom are negative whereas the remaining one carbon atom is positively charged in the title compound. The oxygen atoms have more negative charges whereas all the hydrogen atoms have the positive charges. The more positive charge of carbon is found for the title compound is C7 and N15 it is mainly due to the substitution of negative charge of oxygen atom and the more positive charge of nitrogen is found for the title compound is N15; it is also mainly due to the substitution of negative charge of two oxygen atoms with nitrogen atom. Illustration of atomic charge plotted for B3LYP/cc-pVDZ and cc-pVTZ levels have been shown in Fig.8.

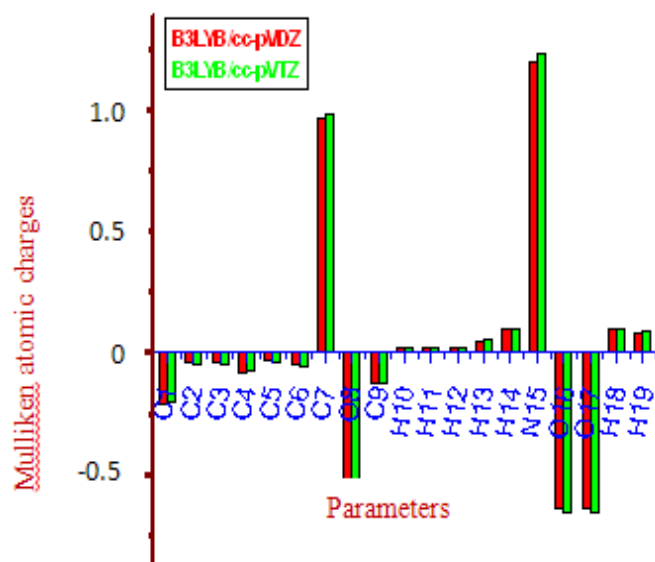


Fig 8. mulliken atomic charges of 1(4-Nitrophenyl)ethane

13. Fukui function

Fukui indices are, in short, reactivity indices, they give us information about which atoms in a molecule have a larger tendency to either loose or accept an electron, which we chemist interpret as which are more prone to undergo a nucleophilic or an electrophilic attack, respectively. The Fukui function is defined by R.G Parr [60] as

$$F(r) = (\delta\rho(r)/\delta(N))r$$

Where $\delta(r)$ is the electronic density, N is the number of electrons and r is the external potential exerted by the nucleus.

Table 7.The DFT/ B3LYP/cc-pVDZ and B3LYP/cc-pVTZ calculated electric dipole moments (Debye), Dipole moments compound, polarizability (in a.u), β components and β_{tot} (10^{-30} esu) value of (4-Nitrophenyl)ethanone

Parameters	B3LYP/ P/ cc-pVDZ	B3LYP/ P/ cc-pVTZ	Parameters	B3LYP/ P/ cc-pVDZ	B3LYP/ P/ cc-pVTZ
μ_x	2.798	2.861	β_{xxx}	36.426	38.746
μ_y	2.124	2.245	β_{yyy}	-1.169	-0.577
μ_z	0.001	0.000	β_{zzz}	-0.001	0.000
μ_{tot}	3.513	3.636	β_{xyy}	-3.322	-3.802
α_{xx}	-85.313	-87.382	β_{xxy}	27.788	30.221
α_{yy}	-66.031	-66.507	β_{xxz}	0.006	0.002
α_{zz}	-67.682	-68.270	β_{xzz}	-7.265	-6.978
α_{xy}	8.892	9.541	β_{yzz}	-0.749	-0.489
α_{xz}	0.003	0.001	β_{YYZ}	0.001	0.000
α_{yz}	-0.002	-0.001	β_{XYZ}	-0.004	0.000

(evaluated from Mulliken population, electrostatic derived charges, etc) at the j^{th} atomic site is the neutral (N), anionic (N+1) or cationic (N-1) chemical species. P.K Chattaraj [63] has introduced the concept of generalized philicity.

Fukui function (FF) is one of the widely used local density functional descriptors to model chemical reactivity and selectivity. The Fukui function is local reactivity descriptors that indicate the preferred where a chemical species will change its density when the number of the electron is modified. Therefore, it indicates the propensity of the electronic density to perform at a given position upon accepting or donating electron [61-62]. Also, it is possible to define the corresponding condensed or atomic Fukui functions on the j^{th} atom site as,

$$F_j^+ = q_j(N+1) - q_j(N)$$

$$F_j^- = q_j(N) - q_j(N-1)$$

$$F_j^0 = \frac{1}{2}[q_j(N+1) - q_j(N-1)]$$

Where f_j^+ and f_j^- describe the ability of an atom to accommodate an extra electron or to cope with lose of an electron and f_j^0 is then considered as an indicator for radical reactivity on the reference molecule. In these equations, q_j is the atomic charge

It contains almost all information about hitherto known different global and local reactivity and selectivity descriptor, in addition to the information regarding the electrophilic / nucleophilic power of a given atomic site in a molecule. Morel et al., [64] have recently proposed a dual descriptor ($\Delta f(r)$), which is defined as the difference between the nucleophilic and electrophilic Fukui function and is given by the equation,

$$\Delta f(r) = [f^+(r) - f^-(r)]$$

$\Delta f(r) > 0$, then the site is favored for a nucleophilic attack, whereas if $\Delta f(r) < 0$, then the site may be favored for an electrophilic attack. According to the dual descriptor $\Delta f(r)$ provide a clear difference between nucleophilic and electrophilic attack at a particular site with their sign.

That is they provide positive value for sited prone for nucleophilic attack and a negative value prone for electrophilic attack. From the values are reported in Table 11. According to the condition for the dual descriptor, nucleophilic sites for in our title molecule are C1, C3, C5, O8, C9, H11, H13, N15 (positive value i.e. $\Delta f(r) > 0$). Similarly, the electrophilic sites are C2, C4, C6, C7, H10, H12, H14, O16, O17, H18, H19 (Negative i.e. $\Delta f(r) < 0$). The behavior of molecule as an electrophilic and nucleophilic attack during reaction depends on the local behavior of the molecule.

Table 8.Quantum Chemical Parameters of 1(4-Nitrophenyl)ethanone calculated at B3LYP/cc-pVDZ and B3LYP/cc-pVTZ level of theory.

Quantum Chemical Parameters	B3LYP/ CC-pVDZ (eV)	B3LYP/ CC-pVTZ (eV)
Ionisation potential(I)= (-Homo energy)	7.3826	7.5804
Electron Affinity(A)= (-Lumo Energy)	2.9665	3.1704
Homo-Lumo Energy gap	-4.4161	-4.4101
Hardness(η)=0.5*(I-A)	2.2080	2.2050
Electronegativity(X)=(I+A)/2	5.1746	5.3754
softness (σ) =1/ η	0.4529	0.4535
Chemical potential(M) = -X	-5.1746	-5.3754
GlobalElectrophilicity(w) = (M*M)/ η^2)	6.0634	6.5520

Table 9.Magnetic susceptibility of 1(4-Nitrophenyl)ethanone at various temperatures.

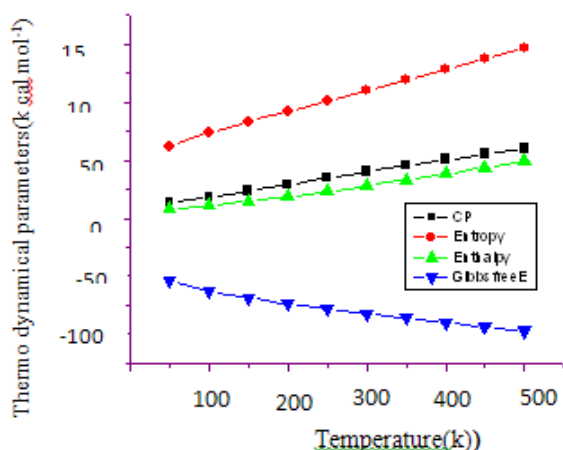
S.No.	Temp. (kelvin)	Susceptibility(χ_m) mole per m^3	1/Temp. (Kelvin ⁻¹)
1	50	1.981E-06	0.0200
2	100	9.907E-07	0.0100
3	150	6.605E-07	0.0067
4	200	4.953E-07	0.0050
5	250	3.963E-07	0.0040
6	300	3.302E-07	0.0033
7	350	2.831E-07	0.0029
8	400	2.477E-07	0.0025
9	450	2.202E-07	0.0022
10	500	1.981E-07	0.0020
11	550	1.801E-07	0.0018
12	600	1.651E-07	0.0017
		5.12379E-07	

Table 10.Mulliken population analysis of 1(4-Nitrophenyl)ethanone performed at B3LYP/cc-pVDZ and B3LYP/cc-pVTZ

Atoms	Atomic charges		Atoms	Atomic charges	
	B3LYP/ cc-pVDZ	B3LYP/ cc-pVTZ		B3LYP/ cc-pVDZ	B3LYP/ cc-pVTZ
C1	-0.210	-0.200	H10	0.021	0.021
C2	-0.036	-0.049	H11	0.021	0.021
C3	-0.043	-0.049	H12	0.019	0.021
C4	-0.083	-0.071	H13	0.048	0.053
C5	-0.029	-0.037	H14	0.096	0.100
C6	-0.049	-0.056	N15	1.198	1.229
C7	0.965	0.983	O16	-0.637	-0.656
O8	-0.692	-0.716	O17	-0.639	-0.658
C9	-0.128	-0.126	H18	0.096	0.100
			H19	0.084	0.088

14. Thermodynamic properties

For the title compound, the standard thermodynamic functions: heat capacity ($C_{p,m}^0$), entropy (S_m^0) and enthalpy (H_m^0), Gibb's free energy (G_m^0) were calculated based on the vibrational analysis by B3LYP method with cc-pVDZ and cc-pVTZ basis sets and statistical thermodynamics were obtained and listed in Table 12.



It is noted from Table 12 that the standard heat capacities, entropies and enthalpies increase from 0 to 500 K because of the intensities of molecular vibration increase with the increasing temperature. According to the data in Table 12 for the title compound, the corresponding relations between the thermodynamic properties heat capacity, entropies, enthalpies, and temperature are described and shown in Fig.9.

15. Conclusion

The vibrational properties of 1(4-nitrophenyl)ethanone have been investigated using experimental techniques (FT-IR and FT-Raman) and density functional theory employing B3LYP exchange-correlation. The theoretically vibrational wavenumbers were compared with the experimental values, which yield good agreement with the calculated values. The complete assignments of fundamental modes were performed on the basis of potential energy distribution. The magnetic properties of the title compound are observed and calculated using GIAO procedure ¹H, ¹³C NMR chemical shifts are compared with experimental data and show a good agreement. The NBO analysis shows the strong intermolecular hyper conjugative interaction of π -electrons in the molecule leading to stabilization of the molecule. From the molecular electrostatic potential plot, it is evident that the negative charge covers the carbonyl and nitro group and the positive region is over the remaining groups and it (MEP) predicts that the carbonyl group and the NO₂ group are most reactive sites for nucleophilic and electrophilic attacks, respectively. Fukui f^+ function recognize carbon atoms of the benzene ring and the area in near vicinity of oxygen atom as possible reaction centers because electron density is gained there as a consequence of the nucleophilic attack. On the other side, Fukui f^- function recognizes the area as possible reaction centers, since NPE molecule loses their electron density when it is under electrophilic attack. In the title compound, the HOMO of π nature is delocalized over the whole C-C bonds of the phenyl ring, and C=O groups. This along with the lowering of HOMO-LUMO band gap supports for the bioactivity of the molecule. Quantum chemical parameters arrived at the frontier molecular orbital theory.

The calculated first hyperpolarizability of the title compound is 2.73×10^{-30} esu, and 21 times that of the standard NLO material urea and the title compound is an attractive object for future studies of nonlinear optical properties.

Acknowledgment

The authors thankful to Sophisticated Analytical Instrumentation Facility (SAIF)-IIT Madras, Chennai for spectral measurement and one of the authors M.Karunanidhi acknowledges the UGC, Ministry of HRD, Govt. of India, for assistance in the form of Minor Research Project. [UGC-SERO-NO.F.MRP-6116/15].

References

- [1]X. Zhang, L. Shan, H. Huang, X. Yang, X. Liang, A. Xing, H. Huang, X. Liu, J. Su, W. Zhang, J. Pharm. Biomed. Anal. 49 (2009) 715–725.
- [2]Z. Liu, Y. Sun, J. Wang, H. Zhu, H. Zhou, J. Hu, J.Wang, Sep.Purif. Technol. 64 (2008) 247-252.
- [3] Y.R. Prasad, A.S. Rao, R. Rambabu, Asian J. Chem. 21(2009) 907-914.
- [4]S. Cacchi, G.Fabrizi, F. Gavazza, A. Goggiamani, Org. Lett. 5 (2003) 289-291.
- [5]P.M. Sivakumar, G. Sheshayan, M.Doble, Chem.Biol.Drug Des.72 (2008) 303-313.
- [6]A.M.Balan, O.Florea, C. Moldoveanu, G. Zbancioc, D. Iurea, I.I. Mangalagiu, Eur.J. Med. Chem. 44 (2009) 2275-2279.
- [7]V.P. Singh, S. Sing, A. Katiyar, J. Enzyme Inhib.Med. Chem. 24(2009) 577-588.
- [8] V.P. Singh, A. Katiyar, S. Sing, Biometalsm21(2008) 491-501.
- [9]H.Z. Wei, L.C. Wing, H.L. Yuan, S.S. Yau, C.L.Yong, H.Y. Chi, Heterocycles. 45 (1997) 71-75.
- [10]M.J.Climent, A. Corma, S. Iborra, A. Velty, J. Catal. 221 (2004) 474-482.
- [11]R.N. Griffin, photochem. Photobiol. 7 (1968) 159-163.
- [12]L Lindqvist, J. Phys.Chem. 76 (1972) 821-825.
- [13]P. Anbusrinivasan, S. Kavitha, Asian J. Chem. 20 (2008) 979-982.
- [14]M. Frisch, G.W. Trucks, H.B. Schlegel, G.E. Scuseria, M.A. Robb, J.R. Cheesman, V.G. Zakrzewski, J.A. Montgomery, Jr., R.E. Strtmann, J.C. Burant, S. Dapprich, J.M.Milliam, A.D. Daniels, K.N. Kudin, M.C. Strain, O. Farkas, J. Tomasi, V. Barone, M. Cossi, R. Camme, B. Mennucci, C. Pomelli, C. Adamo, S. Clifford, J. Ochterski, G.A. Petersson, P.Y. Ayala, Q. Cui, K. Morokuma, N. Rega, P. Salvador, J.J.Dannenber, D.K. Malich, A.D. Rabuck, K. Raghavachari, J.B. Foresman, J.Cioslowski, J.V. Ortiz, A.G. Baboul, B.B. Stetanov, G. Liu, A. Liashenko, P. Piskorz, I. Komaromi, R. Gomperts, R.L. Martin, D.J. Fox, T. Keith, M.A. Al-Laham, C.Y.Peng, A. Nsnsyskkara, M. Challacombe, P.M.W. Gill, B. Johnson, W. Chen, M.W.Wong, J.L. Andres, C. Gonzalez, M. Head-Gordon, E.S. Replogle, J.A. Pople, GAUSSIAN 09, Revision A.02, Gaussian, Inc, Pittsburgh, PA, 2009.
- [15]J.B.Foresman, in: E. Frisch (Ed), Exploring chemistry with Electronic Structure Methods: A Guide to Using Gaussian, Pittsburg, PA, 1996.
- [16]R.Dennington, T. Keith, J. Millam, Gaussview, Version 5, semichem Inc., ShawneeMission KS, 2009.
- [17]T. Sundius, J. Mol. Struct. 218 (1990) 321.
- [18]T. Sundius, Vib. Spectrosc. 29 (2002) 89.
- [19]P.L. Polavarapu, J. Phys. Chem. 94 (1990) 8106.

- [20]G. Keresztury, S. Holly, J. Varga, G.A. Besenyei, Y. Wang, J.R. Durig, *Spectrochim. Acta Part A* 49A (1993) 2007.
- [21]G. Keresztury, *Raman Spectroscopy: Theory in: J.M. Chalmers, P.R. Griffiths (Ed.), Hand book of Vibrational Spectroscopy*, vol. 1, Wiley, 2002.
- [22]N.P.G. Roeges, *A Guide to the complete interpretation of IR Spectra of Organic compounds*, Wiley, New York, 1994.
- [23]A. Raj, Y.S. Mary, C.Y. Panicker, H.T. Varghes, K. Raju, *Spectrochim. Acta* 113 (2013) 28-36.
- [24] N. Sundaraganesan, S. Ayyappan, H. Uma Maheshwari, B.D. Joshua, *Spectrochim. Acta* 66 (2007) 17-27.
- [25]R.M. Silverstein, F.X. Webster, *Spectrometric Identification of Organic Compounds*, sixth ed., John Wiley Asia, 2003.
- [26]C.Y. Panicker, H.T. Varghes, V.S. Madhavan, S. Mathew, J.Vinsova. C.V. Alsenoy, Y.S. Mary, *J. Raman Spectrosc.* 40 (2009) 2176-2186.
- [27] S. Sebastian, N. Sundaraganesan, *Spectrochim. Acta* 75 (2010) 941-952.
- [28] N.B Colthup, L.H. Daly, S.E. Wiberly, *Introduction to IR and Raman spectroscopy*, Academic Press, New York, 1990
- [29]S.Gumus, T. Sundius, V.T. Yilmaz, *spectrochim. Acta* 98 (2012) 384-395.
- [30]G. Varsanyi, *Assignments for Vibrational Spectra of Seven Hundred Benzene Derivatives*, Wiley, New York, 1974.
- [31]M.Kaur, Y.S. Mary, H.T. Varghes, C.Y. Panicker, H.S. Yathirajan, M.S. Siddegowda, C. Van Alsenoy, *Spectrochim. Acta* 98 (2012) 91-98.
- [32]Y.S.Mary, K.Raju, I.Yildiz, O.Temiz-Arpaci, H.I.S. Nogueira, C.M.Granadeiro, C.Van Alsenoy, *Spectrochim. Acta* 96 (2012) 617-625.
- [33]I.Sidir, Y.G.Sidir, E.Tasal, C.Ogretir, *J. Mol. Struct.* 980 (2010) 230-244.
- [34]E. Inkaya, M. Dincer, E. Korkusuz, I. Yildirim, *J. Mol. Struct.* 2013 (2012) 67-74.
- [35]T.Rajamani, S.Muthu, *Solid State Sci.* 16 (2013) 90-101.
- [36]A.F.Holleman, E.Wiberg, N.Wiberg, in: W.de Gruyter (Ed.), *Lehrbuch der Anorganischen Chemie*, Berlin, New York, 2007.
- [37] Jerry P. Jasinski, Ray J. Butcher, A. S. Praveen, H. S. Yathirajan, B. Narayana, *Acta Cryst. E* 67 (2011) 029-030.
- [38] K.Wolinski, J.F.Hinton, P.Pulay, *J. Am. Chem. Soc.* 112 (1990) 8251.
- [39]N.Okulik, A.H.Juber, *Internet Electron. J. Mol. Des.* 4 (2005) 273.
- [40]P.Politzer, J.S. Murray, *Rev. Comput. Chem.* 2 (1991) 273.
- [41]Y.R.Shen, *The Principles of Nonlinear Optics*, Wiley, New York, 1984.
- [42]P.V.Kolinsky, *Opt. Eng.* 31(1992) 1676-1684.
- [43]D.F.Eaton, *Science* 25 (1991) 281-287
- [44]D.A.Kleinman, *Phys. Rev.* 126 (1962) 1977-1979.
- [45]C.Adant, M.Dupuis, J.L.Bredas, *Int. J. Quantum CHEM.* 56 (1995) 497-507.
- [46]G.Purohit, G.C. Joshi, *Indian J. Pure Appl. Phys.* 41 (2003) 922-926.
- [47]A.J.Camargo, H.B.Napolitano, J.Zukerman-Schpector, *J. Mol. Struct. Theochem* 816 (2007) 145-151.
- [48]E.D.Glendening, A.E.Reed, J.E.Carpenter, F.Weinhold, NBO Version 3.1, Gaussian Inc., Pittsburgh, PA, 2003
- [49]A.E.Reed, L.A.Curtiss, F.Weinhold, *Chem.Rev.* 88 (1988) 899-926.
- [50]C.G.Liu, Z.M.Su, X.H.Guan, S.Muhammad, *J. Phy. Chem.* 115c (2011) 23946-23954.
- [51]N.Choudhary, S.Bee, A.Gupta, P.Tandon, *Comp. Theor. Chem.* 1016 (2013) 8-21.
- [52]K.Fukui, T.Yonezawa, H.Singu, *J. Chem. Phy.* 20 (1952) 722-725.
- [53]L.Sinha, O.Prasad, V.Narayan, S.R. Shukla, *J. Mol. Simul.* 37 (2011) 153-163.
- [54]D.F.V. Lewis, C. Ioannides, D.V Parke, *Xenobiotica* 24 (1994) 401-408.
- [55]B. Kosar, C.Albayrak, *Spectrochim. Acta.* 78A (2011) 160-167.
- [56]A.G.Al-Sehemi, A.Irfan, *Arab. J. Chem.* Doi: 10.1016 / j.arabjc.2013.06.019.
- [57]R.G.Parr, R.G.Pearson, *J. Am. Chem. Soc.* 105 (1983) 7512-7516.
- [58]M.C Gupta, *Atomic and Molecular Spectroscopy*, New Age International Private Limited, Publishers, New Delhi, 2001.
- [59]J.P.Foster, F.Weinhold, *J. Am. Chem. Soc.* 102 (1980) 7211-7218.
- [60]R.G.Parr, W.Yang, *Density functional Theory of Atoms and Molecules*, Oxford University Press, New York, 1989.
- [61]P.W.Ayers, R.G.Parr, *J. Am. Chem. Soc.* 122 (2000) 2010-2018.
- [62]R.G.Parr, W.Yang, *J. Am. Chem. Soc.* 106 (1984) 511-516.
- [63]P.K.Chattaraj, B.Maiti, U.Sarkar, *J. Phys. Chem. A* 107 (2003) 4973-4975.
- [64]C.Morell, A.Grand, A.Toro-Labbe, *J.Phys.Chem. A* (2005)205-212.